

## 4 Surface/Interface Project – Crystalline, magnetic and electronic structures at the surface and interface of magnetic thin films and multilayers –

Project Leader: Kenta Amemiya

### 4-1 Introduction

The surface and interface of magnetic thin films play essential roles in the appearance of extraordinary magnetic properties such as perpendicular magnetic anisotropy and the giant magnetoresistance effect. We are investigating the crystalline, magnetic and electronic structures at the surface and interface of magnetic thin films and multilayers, in order to reveal the origin of fascinating magnetic properties, which cannot be realized in bulk materials. The subjects of our study include: magnetic anisotropy of Fe/Ni multilayers [1,2], magnetism at the interface between MgO and Heusler alloy [3], effects of ion irradiation on ultrathin films [4,5], and magnetic depth profile of Gd/Cr multilayers, mainly by means of the X-ray magnetic circular dichroism (XMCD) technique. Moreover, neutron reflectivity experiments have started at BL-17 in J-PARC. We also plan to perform muon spin rotation experiments using an ultra-slow muon source.

### 4-2 Experimental technique: Polarized neutron reflectivity experiment at BL-17 in J-PARC

Polarized neutron reflectivity (PNR) is one of the most powerful techniques for investigating the magnetic depth profile of thin films and multilayers. Since PNR is sensitive to the buried interface, it is complementary to XMCD in the soft X-ray region, which is quite surface sensitive with a typical probing depth of a few nm. Recently, a PNR station has been developed at BL-17 in J-PARC (Fig. 1), and we performed a PNR experiment for a Gd/Cr multilayer as the first user of BL-17, in order to observe the magnetic moment in the Cr layer, which is expected to be induced at the interface with ferromagnetic Gd.

Figure 2 shows preliminary data for an  $\text{Al}_2\text{O}_3$  (substrate) / Mo (20 nm) / Cr (2 nm) / [Cr (0.5 nm) / Gd (3 nm)]<sub>15</sub> / Pt (10 nm) multilayer sample, taken at room temperature without external magnetic field by using the unpolarized neutron beam. The overall structure of the reflectivity curve is consistent with the sample configuration, indicating the feasibility of the technique for multilayer samples. Since the Curie temperature of the present sample is  $\sim 70$  K, a low-temperature PNR experiment with a magnetic field of  $\sim 0.5$  T is now under way.



Fig. 1 Polarized neutron reflectivity experiment at BL-17 in J-PARC.

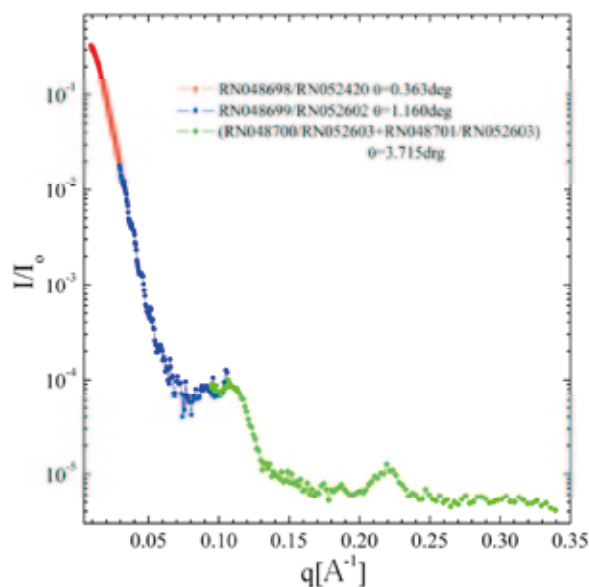


Fig. 2 Neutron reflectivity curve for Gd/Cr multilayer taken at room temperature without external magnetic field.

### 4-3 Scientific Topics (1): Interface magnetism of MgO/Co<sub>2</sub>MnSi tunnel junction [3]

The tunneling resistance in a magnetic tunnel junction (MTJ), a thin insulating layer sandwiched by two ferromagnetic (FM) metallic layers, varies depending on the relative magnetic alignment of the two FM layers, which is called the tunnel magnetoresistance (TMR) effect. It is well understood that the TMR effect is sensitive to the magnetic structure in the interface region between the FM and insulating layers. The thermal fluctuation of interfacial magnetic moments is considered to critically affect the temperature dependence of TMR properties. In fact, it has been reported that MTJs with a Co<sub>2</sub>MnSi (CMS) / MgO structure exhibit a large TMR ratio at low temperature, which reflects the half-metallic nature of CMS, while the TMR ratio shows an unexpected drastic reduction with increasing temperature [6,7]. This seems strange because MTJs with a CoFe/MgO structure show small temperature dependence in the TMR ratio, even though the Curie temperature of CMS is almost the same as that of CoFe.

Although the different temperature dependence of the TMR ratio between the CMS/MgO and CoFe/MgO MTJs must be attributed to the difference in the magnetic structures at the interface, no experimental study has investigated the relationship between the TMR properties and magnetic properties in the actual interface region of MTJs. The depth-resolved XMCD method, in which the probing depth is controlled by using the detection-angle dependence of the effective electron escape depth, is a powerful tool for separately investigating magnetic properties in the actual surface region and in the inner layers of the FM film [8,9]. By using this method for a MTJ structure without an upper FM layer (called a half-MTJ structure here), we can evaluate magnetic moments of the lower FM layer in the region of a few MLs from the interface of the tunneling barrier, MgO. In this study, we applied the depth-resolved XMCD method to half-MTJ films with CoFe/MgO and CMS/MgO structures to investigate the relationship between the TMR properties and interfacial magnetic moments.

Depth-resolved XMCD measurements were performed at BL-7A and 16A in the Photon Factory using an imaging-type microchannel-plate detector with a phosphor screen and a CCD camera, operated in a partial electron yield mode, with an applied retarding voltage of 500 V for preferential collection of Co LMM Auger electrons. A series of XMCD spectra at different probing depths were collected simultaneously for various electron detection angles  $\theta_d$ , as depicted in Fig. 3. The sample was magnetized along the X-ray beam direction using pulsed current through a coil

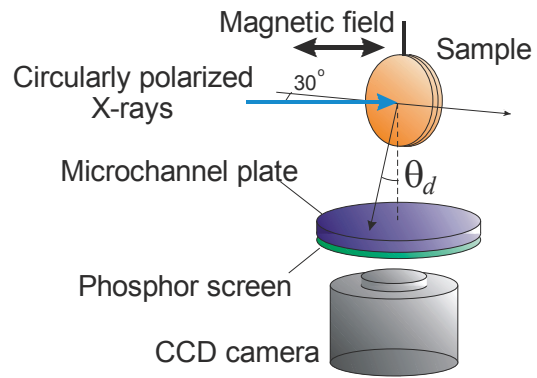


Fig. 3 Schematic layout for the depth-resolved XMCD measurement in the grazing X-ray incidence configuration, which is sensitive to the in-plane magnetic moment.

(about 500 Gauss) and the coil was retracted during the measurement. Since both films exhibit in-plane magnetization, the magnetic moments were determined using XMCD spectra at grazing X-ray incidence, in which the angle between the sample surface and the X-ray beam was 30°.

Figure 4 shows Co L-edge XMCD spectra for CMS/MgO half-MTJ at the interface and in the inner layers, which were extracted from a set of XMCD data at different probing depths taken at room temperature. The effective spin and orbital magnetic moments,  $m_s^{eff}$

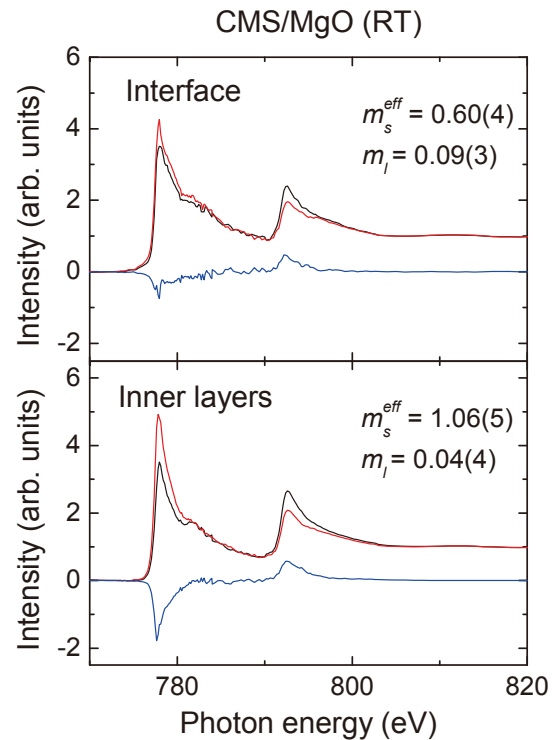


Fig. 4 Co L-edge XMCD spectra of CMS layer at the interface with MgO (top) and in the inner layers (bottom) extracted from a set of XMCD spectra at different probing depths taken at room temperature.

and  $m_p$  were estimated by applying the XMCD sum rules. The effective spin moment,  $m_s^{eff}$ , at the interface is just  $0.60 \mu_B$ , which is 57% of that observed in the inner layers of the CMS. The X-ray absorption spectra of Co and Mn (not shown here) at the interface exhibit no feature suggestive of oxidization at the interface, indicating a high interfacial quality. Therefore, it is considered that there is an intrinsic reason for the large reduction of  $m_s^{eff}$  at the CMS/MgO interface. On the other hand,  $m_s^{eff}$  is also smaller in the interface region of CoFe/MgO, but remains relatively large ( $1.90 \mu_B$ , almost 80% of that in the inner layers), as shown in Fig. 5.

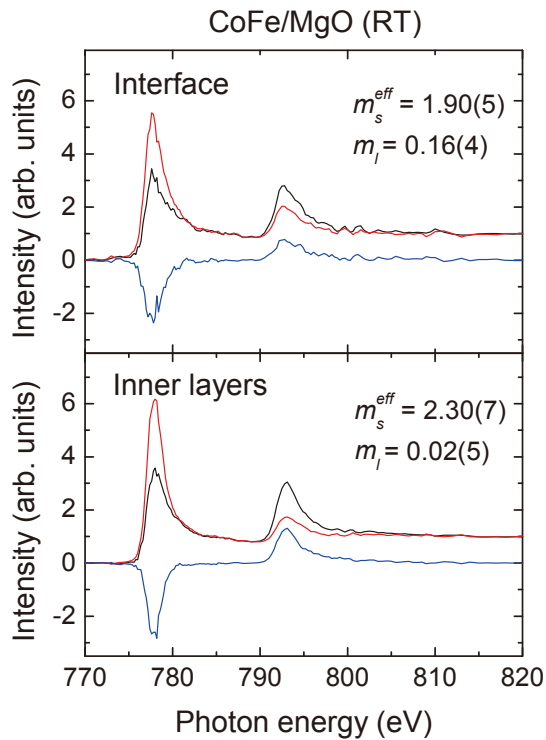


Fig. 5 Extracted Co L-edge XMCD spectra of CoFe layer at the interface with MgO (top) and in the inner layers (bottom) at room temperature.

It is well known that the stiffness,  $A$ , of exchange coupling is proportional to  $JM^2$ , where  $J$  and  $M$  represent the exchange energy and magnetic moment, respectively. Thus, small  $M$  at the interface inevitably results in large thermal fluctuation of the magnetic moment. From a simple estimation of  $A$  in the Co interfacial magnetic moment using the observed  $m_s^{eff}$ ,  $A$  becomes just one-third of that in the inner layers in the CMS/MgO MTJ even when the reduction of  $J$  at the interface is not taken into account. In the first-principles calculation of tunneling conductance with non-collinear spin configuration at the interface taken into consideration, a large reduction of TMR is predicted to occur even by a small tilting of the interfacial magnetic

moments [10]. Since the small exchange stiffness,  $A$ , results in tilting of the magnetic moment at elevated temperature, it is concluded that the large difference in the interfacial magnetic moment in the CoFe/MgO and CMS/MgO structures can qualitatively explain the remarkable difference in the temperature dependence of TMR ratio between them. The weak exchange stiffness indicated from the small  $m_s^{eff}$  of Co at the CMS/MgO interface is the most likely cause of the extremely large temperature dependence of the TMR ratio in the MTJs with CMS electrodes.

Finally, we discuss the temperature dependence of the XMCD data. The XMCD spectrum at the CMS/MgO interface exhibits no remarkable variation even at  $\sim 80$  K as shown in Fig. 6. This seems to contradict the above-discussed temperature dependence of TMR. However, the tiny temperature dependence of  $m_s^{eff}$  in contrast to the large dependence of TMR is reasonably explained as follows: At finite temperature,  $T$ , a magnetic moment thermally fluctuates from the exact easy-axis direction with a certain tilting angle,  $\theta(T)$ , which can be estimated from the exchange stiffness constant,  $A$ , by calculating the Boltzmann average of  $\theta(T)$  against thermal fluctuation energy,  $k_B T$ . By using the calculated  $A$  at the CMS/MgO interface [10],  $\theta(T)$  of the interfacial Co magnetic moments are estimated to be  $12^\circ$  at 80 K and  $22^\circ$  at 300 K. The net reductions of the interfacial Co magnetic moment due to thermal

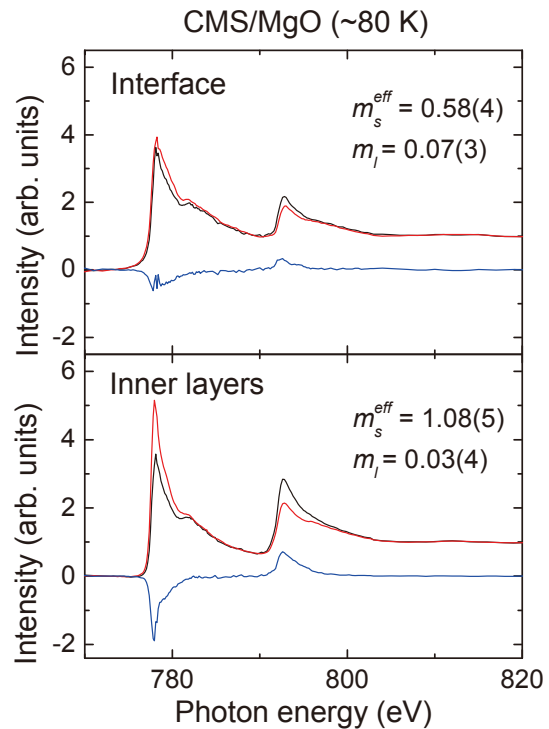


Fig. 6 Extracted Co L-edge XMCD spectra of CMS layer at the interface with MgO (top) and in the inner layers (bottom) at  $\sim 80$  K.

fluctuation from 0 K are  $0.02 \mu_B$  at 80 K and  $0.07 \mu_B$  at 300 K, indicating a tiny reduction of the magnetic moment from 80 to 300 K even when we consider a drastic decrease of  $A$  at the MgO interface. Therefore, it is understandable that there is no remarkable temperature dependence of  $m_s^{eff}$  from 80 to 300 K in our XMCD measurements, not only in CoFe/MgO but also in CMS/MgO half-MTJs. In stark contrast, the TMR ratio is predicted to be reduced strongly even by a tiny  $\theta(T)$  in the CMS/MgO MTJ because of the creation of spin-flipping conductance at the interfacial region [10].

#### 4-4 Scientific Topics (2): Origin of ion irradiation-induced perpendicular magnetization [5]

Much effort has been made to realize perpendicular magnetic anisotropy (PMA) in thin films and multilayers, especially in view of their application to high-density magnetic recording media. Among them, the control of magnetic anisotropy by ion irradiation has attracted much interest in the last decade, due to the possibility of nanostructure patterning by using a focused ion beam. In fact, a Ga<sup>+</sup>-induced spin reorientation transition to perpendicular magnetization from in-plane magnetized Pt/Co/Pt thin films has recently been reported [11,12]. However, the origin of the ion-induced appearance of PMA is not yet understood structurally, though the lattice distortion must play a key role in the determination of magnetic anisotropy. We have clarified the Ga<sup>+</sup> irradiation-induced changes in magnetic anisotropy and crystalline structure of a Pt/Co/Pt ultrathin film by means of XMCD and extended X-ray absorption fine structure (EXAFS) techniques.

Co L-edge XMCD spectra were taken at BL-16A in the Photon Factory, at room temperature in the total-electron-yield mode. The XMCD measurements were performed both in an applied magnetic field of 1.2 T and in the remanent state after magnetizing the sample with a magnetic field pulse of  $\sim 0.05$  T. We adopted the normal and grazing incidence configurations for the XMCD measurements, in order to examine magnetic anisotropy of the film. The Co K-edge EXAFS spectra were measured at BL-12C in the Photon Factory, at 20 K in the fluorescence-yield mode with a 19-element solid-state detector. To examine crystallographic anisotropy in the Co thin film, the EXAFS spectra were taken at normal and grazing incidence configurations. The appearance of PMA was confirmed from the XMCD measurement at remanent magnetization (not shown), at Ga<sup>+</sup> ion fluences of  $1\text{--}2 \times 10^{14}$  ions/cm<sup>2</sup>.

The spin magnetic moment,  $m_s$ , as well as the orbital magnetic moments in the in-plane and out-of-plane directions,  $m_i^{\parallel}$  and  $m_i^{\perp}$ , respectively, are estimated at each ion fluence by applying the angle-dependent sum rules, and are summarized in Fig. 7(a). For the non-irradiated Co film, in which in-plane magnetization is obtained at remanence,  $m_i^{\parallel}$  is slightly larger than or almost the same as  $m_i^{\perp}$ . On the other hand,  $m_i^{\perp}$  is significantly larger than  $m_i^{\parallel}$  at Ga<sup>+</sup> fluence of  $1\text{--}2 \times 10^{14}$  ions/cm<sup>2</sup>, in which PMA is observed. At higher Ga<sup>+</sup> fluences, corresponding to in-plane magnetization again, the difference between  $m_i^{\parallel}$  and  $m_i^{\perp}$  almost disappears. The effective magnetic anisotropy energy,  $K_{eff}$ , of a film is related to the difference between  $m_i^{\parallel}$  and  $m_i^{\perp}$  as expressed by

$$K_{eff} = -2\pi M^2 + F(m_i^{\perp} - m_i^{\parallel}),$$

where  $M$  and  $F$  are the saturation magnetization and a proportionality factor, respectively. By adopting this simple relation, we can estimate  $K_{eff}$  for the Co film. Since various  $F$  values have been reported ranging from 0.7 to 50 meV/ $\mu_B$ , we plot the estimated  $K_{eff}$  for  $F = 1, 2.5,$  and  $5$  meV/ $\mu_B$  in Fig. 7(b). Magnetic anisotropy of the present film is well reproduced by assuming  $F = 1\text{--}5$  meV/ $\mu_B$ , which seems reasonable considering a recent report, in which  $F = 2.0$  and  $3.0$  meV/ $\mu_B$  were obtained for Fe and Ni, respectively [13]. The Ga<sup>+</sup> irradiation-induced changes in magnetic anisotropy are thus interpreted by the changes in anisotropy of the Co orbital moment.

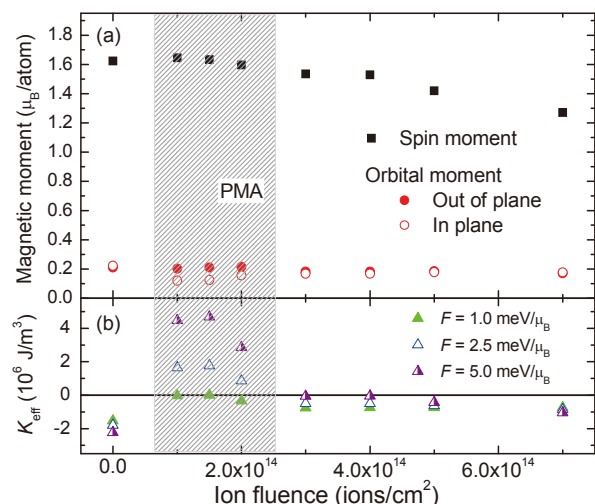


Fig. 7 Spin (black squares) and out-of-plane (filled red circles) and in-plane (open red circles) orbital magnetic moments of Co in a Pt/Co/Pt film (a), together with magnetic anisotropy energy,  $K_{eff}$ , including shape anisotropy, estimated from the orbital moments by assuming indicated proportionality factors,  $F$  (b). A shaded area corresponds to the appearance of PMA.



Figure 8 shows Fourier transforms of the Co K-edge EXAFS function,  $k\chi(k)$ , of a Pt/Co/Pt film with different  $\text{Ga}^+$  ion fluences. For the non-irradiated Co film, a sharp peak at a distance of  $\sim 2 \text{ \AA}$ , which corresponds to the nearest Co-Co bond, is observed. Note that the phase shift effect in EXAFS is not corrected, so the peak appears at a shorter distance than the actual one. With increasing  $\text{Ga}^+$  fluence, the amplitude of the peak rapidly decreases and the peak shifts towards the larger distance, suggesting a reduction of the coordination number and an expansion of the Co-Co bond length. Moreover, another peak appears at  $\sim 2.5 \text{ \AA}$ , which grows with increasing  $\text{Ga}^+$  fluences, directly indicating the contribution from the Co-Pt bond due to the intermixing between Co and Pt.

We further analyze the EXAFS data in order to obtain quantitative structural parameters. In-plane and out-of-plane bond lengths are separately determined by simultaneous fitting of the EXAFS data taken both at normal and grazing incidence configurations. The obtained Co-Co bond lengths are given in Fig. 9 for each  $\text{Ga}^+$  fluence. For the non-irradiated film, the Co-Co bond lengths are almost isotropic and similar to that of bulk hcp Co. In contrast, at a  $\text{Ga}^+$  irradiation of  $1.5 \times 10^{14}$  ions/cm<sup>2</sup>, the in-plane bond length is significantly expanded by 4.8%, while the out-of-plane one shows relatively small expansion of 2.4%. This structural change might be because Co atoms are struck out by  $\text{Ga}^+$  irradiation and/or intermixing with Pt occurs in the vicinity of the Co/Pt interface. In fact, a large coordination number for the Co-Pt bond is obtained for the irradiated film, suggesting significant Co-Pt intermixing. Such a large lattice distortion would enhance PMA through the magnetoelastic effect in the Co film. If we assume the magnetoelastic constants of bulk Co, the obtained lattice distortion results in an increase in the magnetoelastic anisotropy energy by  $2.0 \times 10^6 \text{ J/m}^3$ . This increase is large enough to induce the spin reorientation transition to PMA, because the shape anisotropy,  $-2\pi M^2 = -1.2 \times 10^6 \text{ J/m}^3$  as estimated from the observed spin moment,  $m_s$ .

At higher  $\text{Ga}^+$  fluence of  $4 \times 10^{14}$  ions/cm<sup>2</sup>, the out-of-plane Co-Co bond length expands by 5.0% compared with that for the non-irradiated sample,

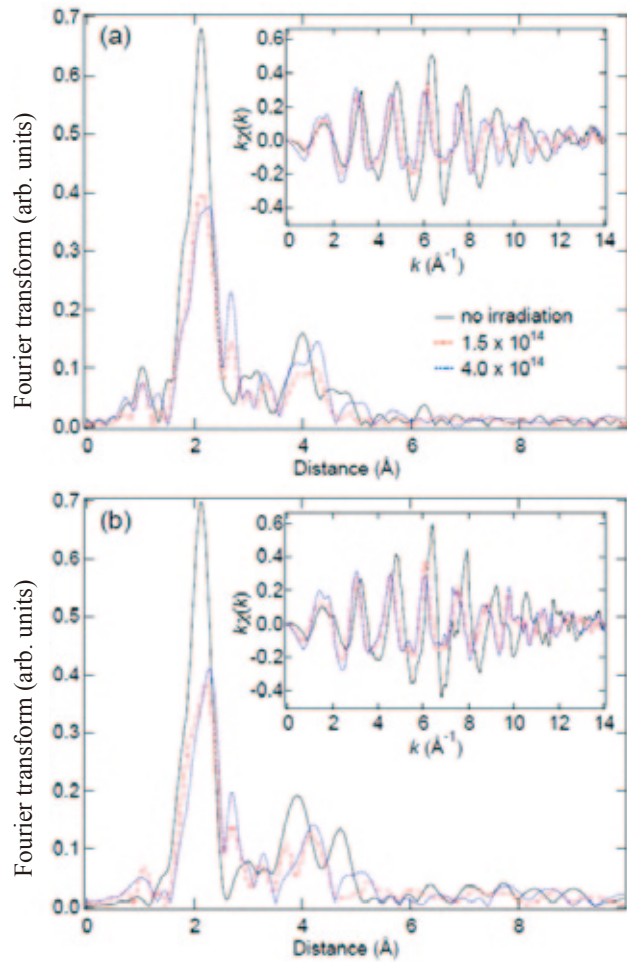


Fig. 8 Fourier transforms of the Co K-edge EXAFS function,  $k\chi(k)$  (inset), of a Pt/Co/Pt film with different  $\text{Ga}^+$  ion fluences, 0 (solid black line),  $1.5 \times 10^{14}$  (dashed red line), and  $4.0 \times 10^{14}$  ions/cm<sup>2</sup> (dotted blue line) taken at the normal (a) and grazing (b) X-ray incidence configurations.

which is now almost the same as the in-plane bond length. Such an isotropic structure would lose PMA. In fact, a similar estimation of the magnetoelastic anisotropy energy yields a decrease of  $0.8 \times 10^6 \text{ J/m}^3$  compared to that estimated at  $\text{Ga}^+$  irradiation of  $1.5 \times 10^{14}$  ions/cm<sup>2</sup>. In addition, the coordination number of out-of-plane Co-Co decreases, while that of out-of-plane Co-Pt increases, indicating that Co-Pt intermixing increases and more Pt atoms exist in the

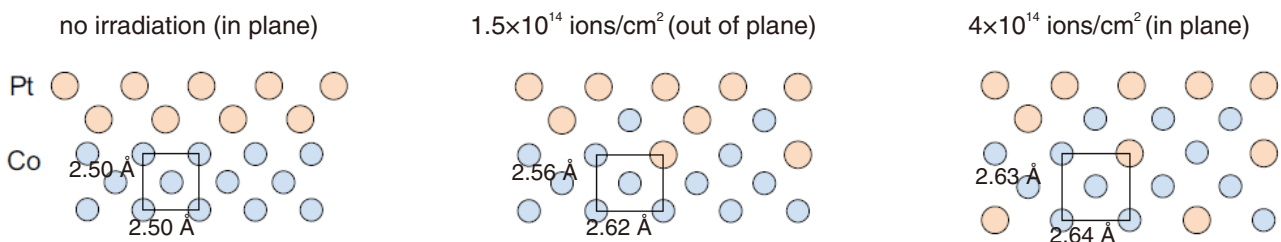


Fig. 9 Crystalline structure and magnetic anisotropy of Pt/Co/Pt thin films irradiated with  $\text{Ga}^+$  ions.

Co layers. Thus, the origin of irradiation-induced changes in magnetic anisotropy is successfully explained by the lattice distortion and Co-Pt intermixing, which were clarified by the EXAFS measurements and XMCD experiment.

- [1] M. Sakamaki and K. Amemiya, *Appl. Phys. Express* 4 (2011) 073002.
- [2] M. Sakamaki and K. Amemiya, *e-J. Surf. Sci. Nanotech.* 10 (2012) 97.
- [3] S. Tsunegi, et al., *Phys. Rev. B* 85 (2012) 180408 (R).
- [4] M. Sakamaki et al., submitted to *Mater. Chem. Phys.*
- [5] M. Sakamaki et al., submitted to *Phys. Rev. B*.
- [6] Y. Sakuraba et al., *Appl. Phys. Lett.* 88 (2006) 192508.
- [7] S. Tsunegi et al., *Appl. Phys. Lett.* 93 (2008) 112506.
- [8] K. Amemiya, *Phys. Chem. Chem. Phys.*, in press.
- [9] K. Amemiya et al., *Appl. Phys. Lett.* 84 (2004) 936.
- [10] Y. Miura et al., *Phys. Rev. B* 83 (2011) 214411.
- [11] J. Jaworowicz et al., *Appl. Phys. Lett.*, 95 (2009) 022502.
- [12] A. Maziewski et al., *Phys. Rev. B* 85 (2012) 054427.
- [13] H. Abe et al., *J. Magn. Magn. Mater.* 302 (2006) 86.